Journal of Materials Chemistry A

RSC Publishing

FEATURE ARTICLE

View Article Online
View Journal | View Issue

Recent progress in organic–inorganic hybrid solar cells

Xia Fan,[a] Mingliang Zhang,[bc] Xiaodong Wang,[b] Fuhua Yang[b] and Xiangmin Meng*[c]

Cite this: *J. Mater. Chem. A*, 2013, **1**, 8694

Received 25th March 2013
Accepted 15th May 2013

DOI: 10.1039/c3ta11200d

www.rsc.org/MaterialsA

Organic–inorganic hybrid solar cells were expected to adopt the advantages of both organic and inorganic materials. Due to several crucial problems, the power conversion efficiency of most hybrid solar cells was lower than 1%. Recent work reported the highest power conversion efficiency of a hybrid solar cell as 11.3%, which increased the research interest into organic–inorganic hybrid solar cells. This article focuses on the progress in state-of-the-art research on organic–inorganic hybrid solar cells and the associated key issues, including the energy band alignment of the organic and inorganic components, interface control of the heterojunction, and the use of ordered nanostructures were discussed. The challenges and prospects for organic–inorganic hybrid solar cells in the near future are discussed.

1 Introduction

So-called 1st generation solar cells based on crystalline and polycrystalline silicon (Si) with power conversion efficiencies (PCE) in the range 18–25% are still dominating the photovoltaics (PV) market. 2nd generation thin film solar cells based on II–VI semiconductors, copper indium gallium selenide (CIGS), and amorphous Si possessed the best PCE of close to 20%.[1] The 3rd generation solar cells were developed to pursue high PCE and low costs for special applications, such as tandem cells, light-condensed cells, organic photovoltaics (OPV), dye-sensitized solar cells (DSSC), organic–inorganic hybrid (OIH) solar cells and so on. Generally, the PCEs and lifetimes of solar cells containing organic components were worse than those of traditional 1st and 2nd generation solar cells. However, the low fabrication cost, flexibility and light weight have made them suitable for several special applications. OIH solar cells could adopt the merits of inorganic materials, such as stability, high carrier mobility and compatible fabricating process, and utilize the advantages of organics, such as enhanced light absorption at a wide range of wavelengths, adjustable molecular structures for energy band alignment, facile solution processability, and so on.

Similar to the Si p–n junction solar cells, the general operating principle of OIH solar cells also involves the following

[a]*Key Laboratory of Bio-Inspired Smart Interfacial Science and Technology of Ministry of Education, School of Chemistry and Environment, Beihang University, Beijing 100191, China*

[b]*Engineering Research Center for Semiconductor Integrated Technology, Institute of Semiconductors, Chinese Academy of Sciences, Beijing 100083, China*

[c]*Key Laboratory of Photochemical Conversion and Optoelectronic Materials, Technical Institute of Physics and Chemistry, Chinese Academy of Sciences, Beijing 100190, China. E-mail: xmmeng@mail.ipc.ac.cn*

Xia Fan received her PhD in organic chemistry from Technical Institute of Physics and Chemistry, CAS, in 2007. She then worked as a senior research associate in City University of Hong Kong, where she studied the synthesis, characterization and application of semiconductor nanomaterials. In 2009, she joined the School of Chemistry and Environment, Beihang University. Her current scientific interests are focused on the design and construction of photoelectric conversional nanomaterials and biomimetic materials and system, especially artificial nanochannels with smart properties.

Mingliang Zhang received his PhD degree in materials chemistry from City University of Hong Kong in 2007. From 2007 to 2009, he worked as a senior research associate in City University of Hong Kong. From 2009 to 2010, he was a post-doctoral research in ECE department of University of California San Diego. He is an associate professor of Engineering Research Center for Semiconductor Integrated Technology at the Institute of Semiconductors, CAS, from 2010. His research interests focused on technologies for micro-/nano-scale fabrication, nanomaterials for energy conversion and MEMS/NEMS devices for chem/biosensors.

steps: light absorption, exciton generation and diffusion, exciton dissociation to carriers at the junction interface and carrier transportation and collection, which is schematically shown in Fig. 1. In the first step, incident photons with energies higher than the band gap of the organic and/or inorganic semiconductors are absorbed and electrons at the ground states are excited. Then, excitons are generated, which are bound electron–hole pairs. Those excitons could diffuse during their lifetime in the organic and/or inorganic semiconductors to their interfaces. With the help of an inner electrical field built by the OIH p–n junction, excitons are dissociated into the holes and electrons at the interface. Next, those charge carriers have to be transported to their respective electrodes to generate an external current. Holes are transported toward the anode electrode through the donor materials, and electrons are transported to the cathode electrode *via* the acceptor materials. Due to the relatively large absorption cross sections of organic semiconductors, light absorption and exciton generation are favorable in OIH solar cells. The exciton diffusion lengths in Si or other inorganic semiconductors could reach several hundred

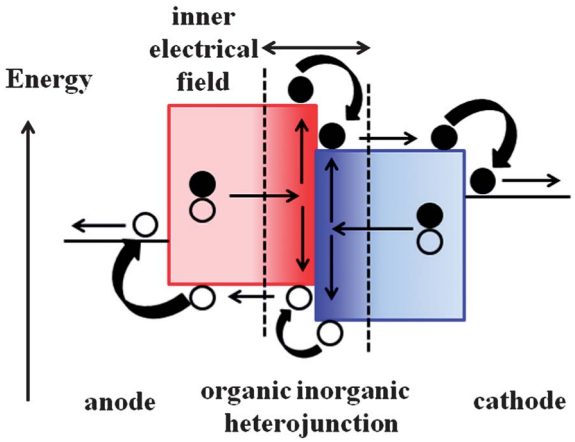

Fig. 1 Scheme of the operating principles of an OIH solar cell, showing the dissociation of excitons and the charge transportation process. The electron (●) and hole (○) transfer processes are indicated with arrows.

nanometers, but the average exciton diffusion lengths are usually shorter than 20 nm in most organic semiconductors,[2–6] which means most of the excitons are quenched before carriers are formed. Excitons in organics have binding energies in the range 200–400 meV,[7,8] which is often higher than the binding energies in most inorganic semiconductor materials, which are in the range 2–40 meV.[9] Thermal energy at room temperature (~25 meV) is not sufficient for exciton dissociation to holes and electrons. Therefore, exciton dissociation must be carried out at the interface with the help of an inner electrical field built by organic and inorganic components with proper highest occupied molecular orbital (HOMO) and lowest unoccupied molecular orbital (LUMO) energy levels. The total area of the interface and the intensity of the inner building electrical field at the interface dominated the exciton dissociation efficiency. Carrier transportation is critical for OIH solar cells. The carrier mobility of most organics is at the level of $\sim 10^{-3}$ m s^{-1} V^{-1}, which is lower than Si by about 5 orders of magnitude. In addition, the carrier collection is also affected by interface state

Xiaodong Wang received his PhD in condensed matter physics from Institute of semiconductor, Chinese Academy of Sciences (CAS) in 2001. Currently, he is a professor/co-director of Engineering Research Center for Semiconductor Integrated Technology at the Institute of semiconductor, CAS. His research experience includes In(Ga)As/GaAs quantum dots lasers, GaInNAs/GaAs quantum well lasers and GaN LEDs. His current research interests are focused on high efficiency solar cells, thermoelectric devices at nanoscale and quantum dot field effect transistor.

Fuhua Yang received his PhD degree in solid physics from Paul Sabatier University, Toulouse in 1998. Currently, he is a professor/director of the Institute of Semiconductors, CAS. His early research involved 2DEG transport, semiconductor cavity optical properties, and light storage device. Now, his research interests include single electron transistor and their integration, RTD/HEMT integrated circuit and MEMS.

Xiangmin Meng earned his bachelor degree in physics from Lanzhou University. Then, he has been a member of the Lab of Atomic Imaging of Solids, Chinese Academy of Sciences (CAS). From 1998 to 1999, as a STA fellow, he worked in National Institute for Materials Sciences, Japan. From 2001 and 2003, he worked in City University of Hong Kong. Since 2005, he became a professor of Technical Institute of Physics and Chemistry, CAS. His current research interests are preparation, structural characterization and property study of semiconductor nanomaterials.

recombination and quenching on dead ends/corners. Due to the increasing number of interface states with increasing interface area, carrier trap and recombination limits the improvement of efficiency. In most OIH solar cells, randomly dispersed inorganic quantum dots (QDs), nanoparticles (NPs), nanocrystals (NCs), nanorods (NRs), nanotubes (NTs) or nanowires (NWs) are blended with organic semiconductors to form a p–n junction. The carriers could not avoid quenching at dead ends/corners on the pathways to their respective electrodes. Therefore, exciton diffusion, dissociation and carrier transportation predominantly affect the performance of OIH solar cells.

For the key issues mentioned above, a lot of effort has been made to improve the performance of OIH solar cells. Based on the interface configuration of p–n junctions, OIH solar cells have been developed by three methods, which are schematically shown in Fig. 2. The deposition of an organic film on an inorganic film can instantly form an OIH solar cell, as depicted in Fig. 2(a). Inorganic QDs, NPs and NWs have been blended with organic semiconductors and OIH solar cells have been fabricated by sandwiching the mixture in between two electrodes, as shown in Fig. 2(b). The junction interface is largely increased and enhanced exciton dissociation can be expected. The main advantage of this configuration is the cost-effectiveness and flexibility of the fabrication process. However, dead-ends and short circuiting of charges could not be avoided in this type of solar cell. In order to further enlarge the interface area and benefit carrier transportation, ordered nanostructures were adopted for use in OIH solar cells, as in Fig. 2(c).

Several reviews have discussed the development and prospects of OIH solar cells. Due to their facile and cost-effective fabrication, the most popular topic was polymer–QDs/NP mixed solar cells, as shown in Fig. 2(b). The fabrication approaches, operation principles and main challenges of this kind of OIH solar cell has been discussed.[10–12] The maximum PCE achieved was about 5% and a theoretical prediction of 10% has been reported.[13,14] Their performance was dominated by the absorption spectra of the active components, the interface morphology of the junction, and the blending composition.[15–18] The synthesis route, dispersed solvents and surface termination of inorganic QDs/NPs also affected the properties of the OIH solar cells.[19] The introduction of proper interfacial materials or tailoring ligands on the QDs/NPs could optimize the optical and electrical properties of the active layer at the interface, and then enhance the performance of OIH solar cells.[20,21] OIH solar cells based on well-ordered nanostructures, as shown in Fig. 2(c), have attracted extensive interest. Large area heterojunctions and regular carrier pathways provided opportunities to develop highly efficient solar cells. Polystyrene sphere template-assisted synthesis can generate several kinds of one-dimensional nanostructured arrays, such as nanopillars, NRs, NWs and NTs.[22] The state-of-the-art research on OIH solar cells based on nanostructured arrays have been reviewed.[23,24]

In order to clearly discuss them, most of the OIH solar cells were categorized into six groups based on the inorganic part used, such as Si, ZnO, TiO_2, II–VI semiconductors, III–V semiconductors and others. The most popular organics for OIH solar cells are summarized in Table 1 and all names have been abbreviated. Based on the large amount of published papers, the energy band diagrams of these frequently used organic and inorganic components, including the electrode materials, are schematically shown in Fig. 3–5. All the abbreviated names of organics can be found in Table 1. The unfilled frame indicates that the energy band varies in that range. The recent progress made in the six kinds of OIH solar cells will be discussed in detail with respect to the planar films, blending with the active layer and ordered nanostructures, as shown in Fig. 2. The energy band alignment, control of the heterojunction interfaces and the performances of several OIH solar cells are discussed. Finally, the challenges and prospects for the near future development of OIH solar cells for practical applications and basic research will be discussed.

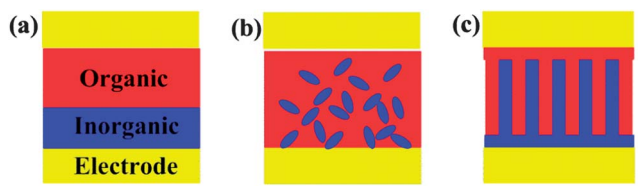

Fig. 2 Scheme of the interface configuration of OIH solar cells: (a) planar films, (b) blending with an active layer and (c) use of ordered nanostructures.

2 Si-based OIH solar cells

Si has been extensively used in solar cell modules and is one of most attractive materials for OIH solar cells. Many papers have reported the PCEs of OIH solar cells with Si which exceeded 10%.[25–29] By far, the highest PCE of an OIH solar cell from the published literature was 11.3%, which was obtained with a device composed of crystalline Si and PEDOT:PSS films containing a 0.1% Zonyl fluorosurfactant as an additive.[30] A schematic of the device and its performance are shown in Fig. 6. The p-type Zonyl-treated PEDOT:PSS was coated on a hydrophobic Si wafer without undergoing any oxidation processes to form the heterojunction. However, the average PCE was decreased by 2 orders of magnitude upon addition of 10% Zonyl fluorosurfactant into the PEDOT:PSS[30] The interface between Si and PEDOT:PSS plays a crucial role in the performance of the OIH solar cell. Compared to a cell with a H-terminated surface, native oxides on the Si surface of suitable thickness could improve the PCE by 530 fold from 0.02% to 10.6%. The native oxide layer had a net positive surface dipole and resulted in a favorable band alignment for charge separation. However, the thick oxide layer at the interface increased the series resistance and degraded the cell performance. It was also found that cells based on (111)-orientated Si demonstrated slightly better performance than that of (100)-orientated Si, as listed in Table 2.[31] When a thin electronic sieve layer of LiF or SiO_x was inserted in the heterojunction of Si and ZnPc, the PCEs of the cells were enhanced from 0.16% to 3.6% and 6.04%, respectively. The potential role of the sieve layer was to block hole diffusion into the acceptor layer of the cell and thereby decrease

Table 1 Molecular structures and abbreviations of the organic semiconductor components in OIH solar cells

Bis-C60-ETM	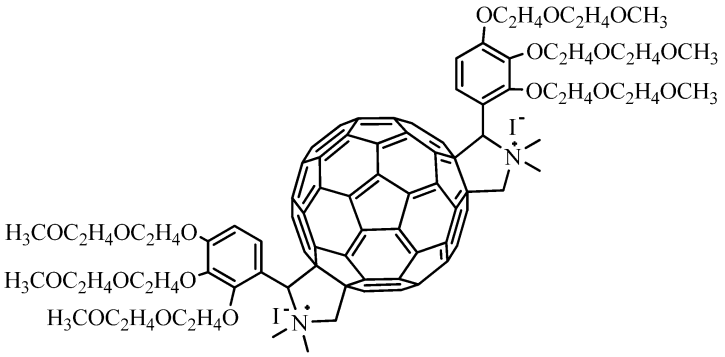
PSSA-*g*-PANI PFI	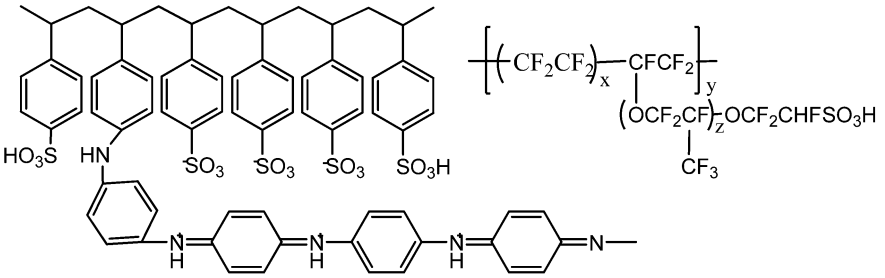
PCBM	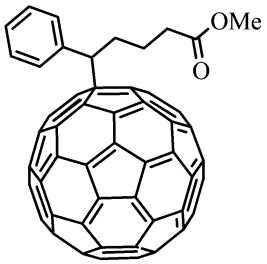
F-PCBM	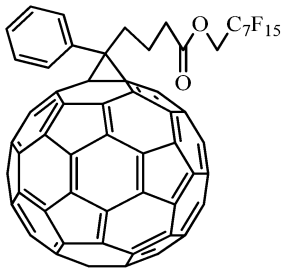
ICBA	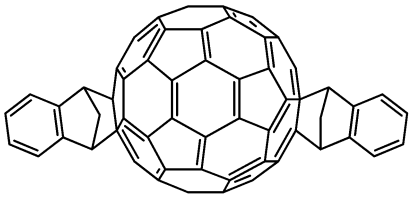
PC71BM	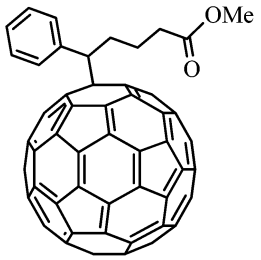
PEG-C60	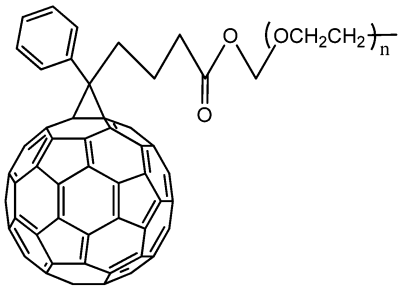
PIDT-PhanQ	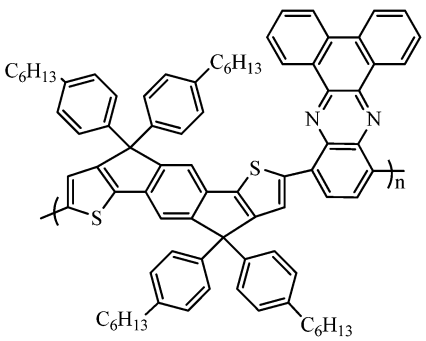

Table 1 (*Contd.*)

X = Cu, CuPc X = Zn, ZnPc	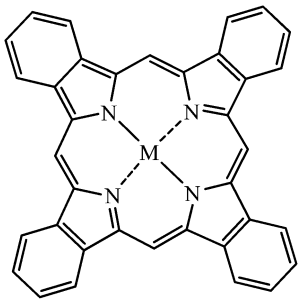	CuPC-ether dye	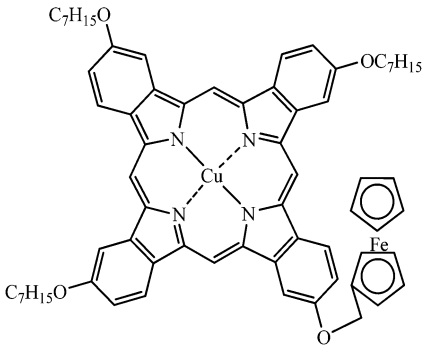
F8T2	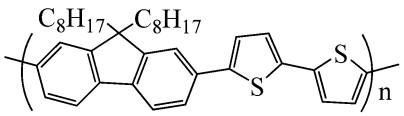	PDOCPDT	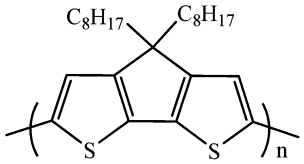
MEH-PPV	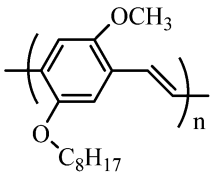	MDMO-PPV	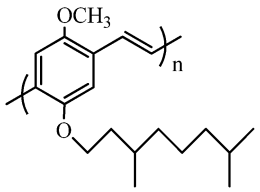
O-3HT-(Br)COOH	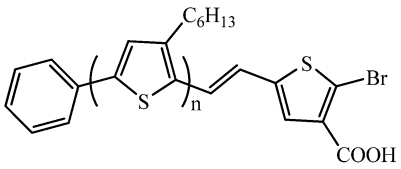	O-C1C10-PPV	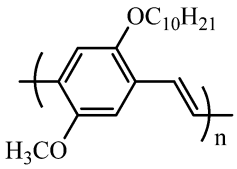
P3HT	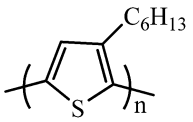	P3TMAHT	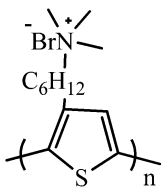
PTEBS	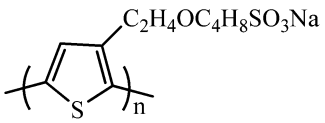	P3OT	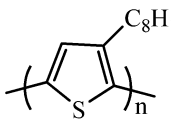
PCDTBT	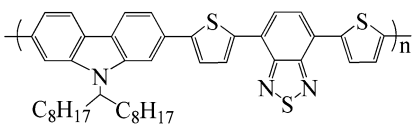	PBTTT	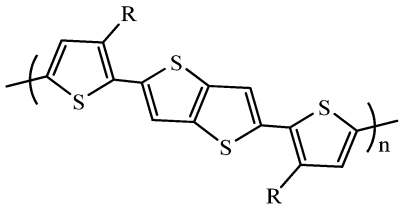
X = C, PCPDTBT X = Si, PSBTBT	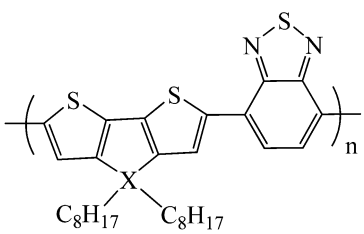	PDDTT	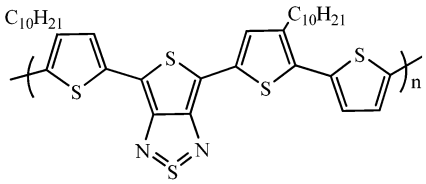

Table 1 (*Contd.*)

X = Si, PDTSTPD X = Ge, PDTGTPD	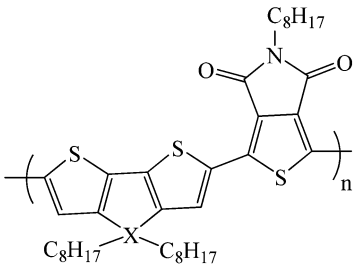	PECz-DTQx	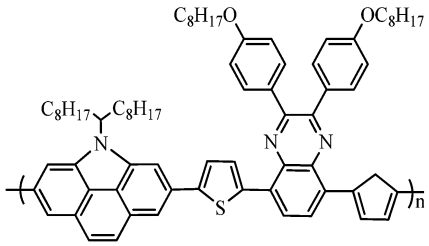
PEDOT:PSS	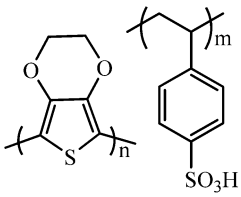	PFN	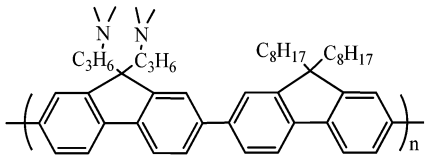
PNDI-1-Th	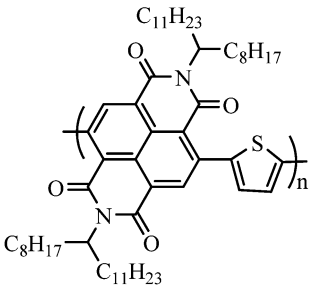	PTAA	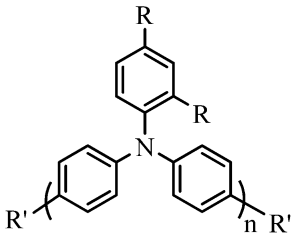
PTB1	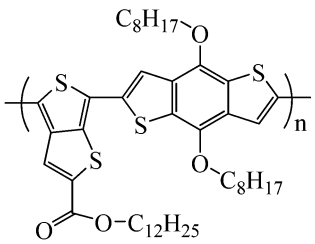	PTB7	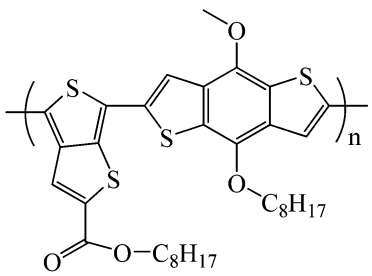
PTV	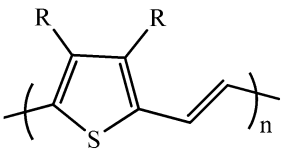	PVK	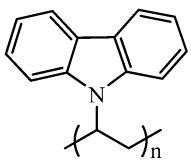
SQ-1	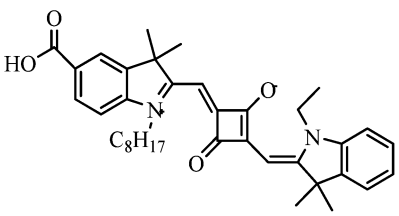	BCP	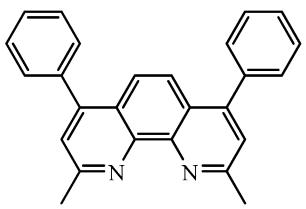

Table 1 (*Contd.*)

SK-1	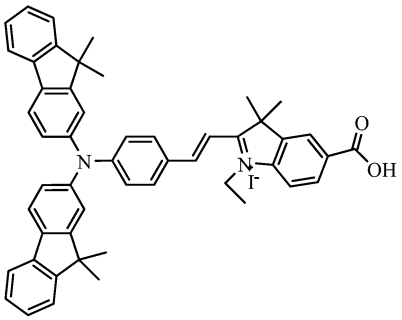	SK-2	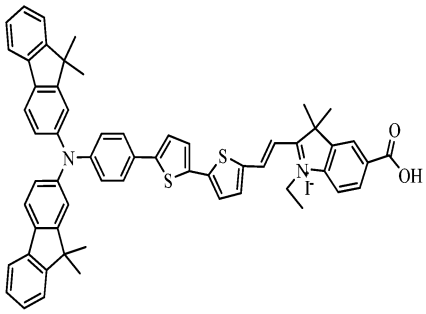
Spiro-OMeTAD	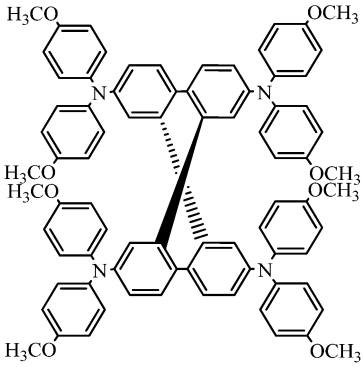	N719	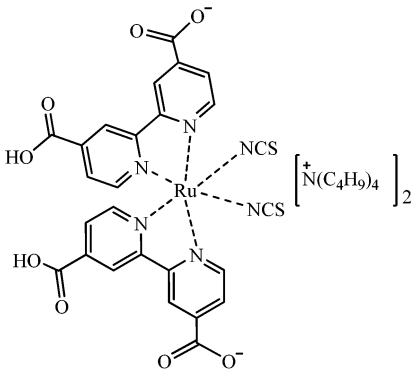

carrier recombination.[32] Considering energy band alignment and effective carrier collection, the organic and inorganic materials should satisfy the following criteria: (1) a low offset between the valence band of the inorganic component and the HOMO of the organic component for a high photocurrent and (2) a large offset between the conduction band of the inorganic component and the LUMO of the organic part for a high open-circuit voltage. The silicon–P3HT interface satisfies these requirements and has demonstrated a PCE of 10.1%.[33] Several kinds of organics have been used for OIH solar cells, such as polyaniline (PANI) mixed with single wall carbon nanotubes (SWCNTs),[34] medicinal compounds[35] and biological macromolecules.[36] The PCEs of those reported cells were lower than 2%. In order to utilize the wide solar spectrum using cost-effective processes, a tandem multijunction OIH solar cell was fabricated with a solution-processed polymer subcell on a hydrogenated amorphous silicon (a-Si:H) subcell. MoO_3 was used as the hole transporting intermediate layer, and the obtained PCE was 1.84% and open-circuit voltage V_{OC} was 1.50 V.[37] Solution-processed OIH solar cells based on SiNWs, SiQDs and polymers, such as P3HT, PEDOT:PSS, MDMO-PPV and PVK, had PCEs of less than 1%.[38,39]

The introduction of ordered Si nanostructures could improve the performance of OIH solar cells though light trapping effects and large heterojunction areas, as well as by forming a 3D interface configuration in the OIH solar cell.[40–46] Compared to cells without a nanowire structure, the PCE of a SiNW–PEDOT OIH solar cell was improved from 0.08% to 5.09%.[47] The frequently used SiNWs in OIH solar cells were fabricated by metal-assisted chemical etching and the length and density of the NWs could be adjusted within a small range. The device made from SiNWs–PEDOT:PSS achieved a PCE of 7.3% when the length and density of SiNW was 2.1 μm and 1×10^8 cm^{-2}, respectively.[48] Other works reported that SiNWs–PEDOT:PSS cells including SiNW with lengths of 0.37, 0.3 and 0.88 μm achieved PCEs of 8.40%, 5.6% and 5.3%.[49–51] For SiNWs–Spiro-OMeTAD OIH solar cells, devices containing SiNW with lengths ranging from 0.15 to 5 μm have been investigated and the cell with NWs of length 0.35 μm possessed the highest PCE of 10.3%.[52–54] When SiNWs were fully embedded inside PEDOT:PSS to form a radial junction, the PCE of the cell was 0.44%. If PEDOT:PSS only covered the top ends of the SiNWs to form an axial junction, the PCE of the cell was 1.82%.[55] However, another paper indicated that compared to an axial junction cell with a PCE of 0.35%, the radial junction cell had a PCE of 4.4%.[56] The amount of interfacial recombination of carriers resulted in the difference. If there is high carrier recombination at the interface, the radial junction cell should be worse than the axial junction cell because of the big interface area. A solar cell composed of Si nanocones with aspect ratios ~1 from drying etching and PEDOT:PSS exhibited a PCE of 11.1%.[57] SiNP modified SiNWs exhibited enhanced light scattering and trapping over a wide range of incidence angles at a wide range of wavelengths. A PCE of 9.2% was achieved based on the solar cell composed of SiNP coated SiNWs and PEDOT:PSS.[58] Upon insertion of PEDOT:PSS, the PCE of a-Si:H nanocones–P3HT:PCBM solar cells was enhanced to 2.22% from 1.73% and the PCE of SiNW–PEDOT:PSS cell was increased greatly from 6.2% to 9%.[59,60] F4-TCNQ doping in P3HT has improved device

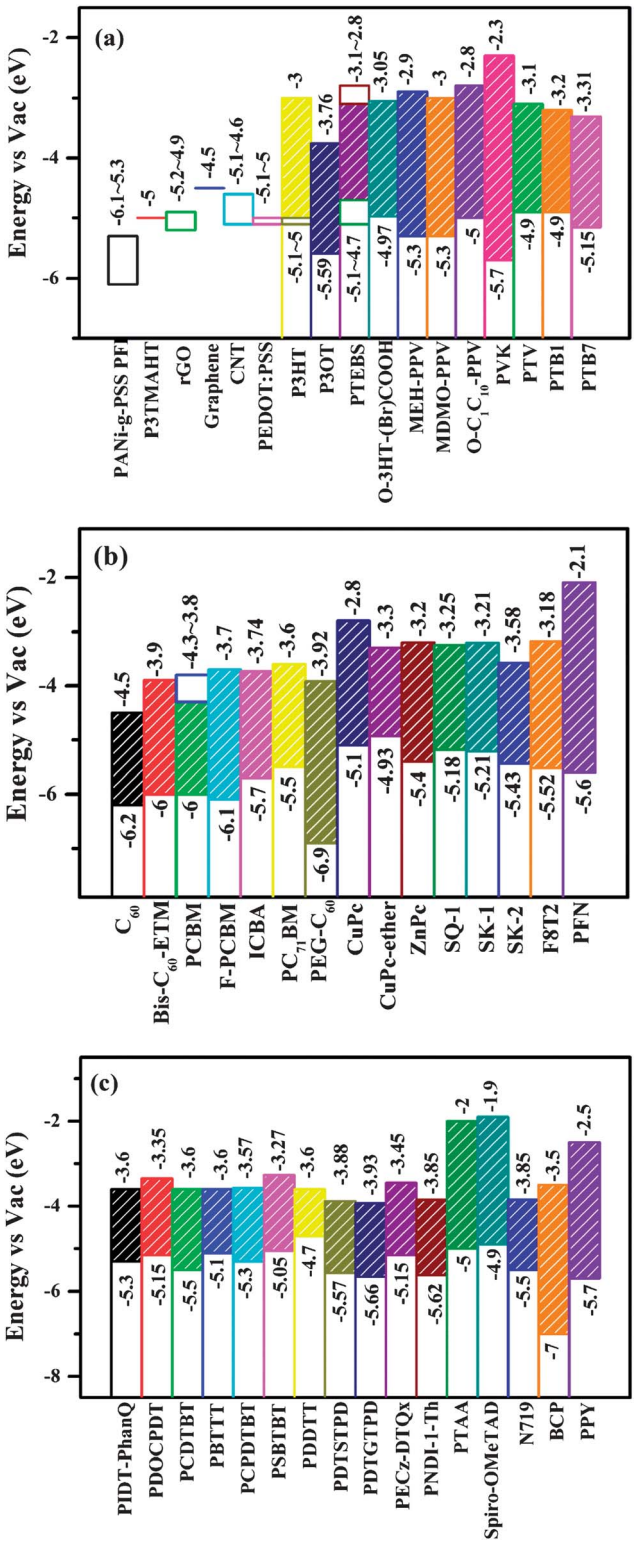

Fig. 3 Schematic of the energy bands of frequently used organics in OIH solar cells (a–c).

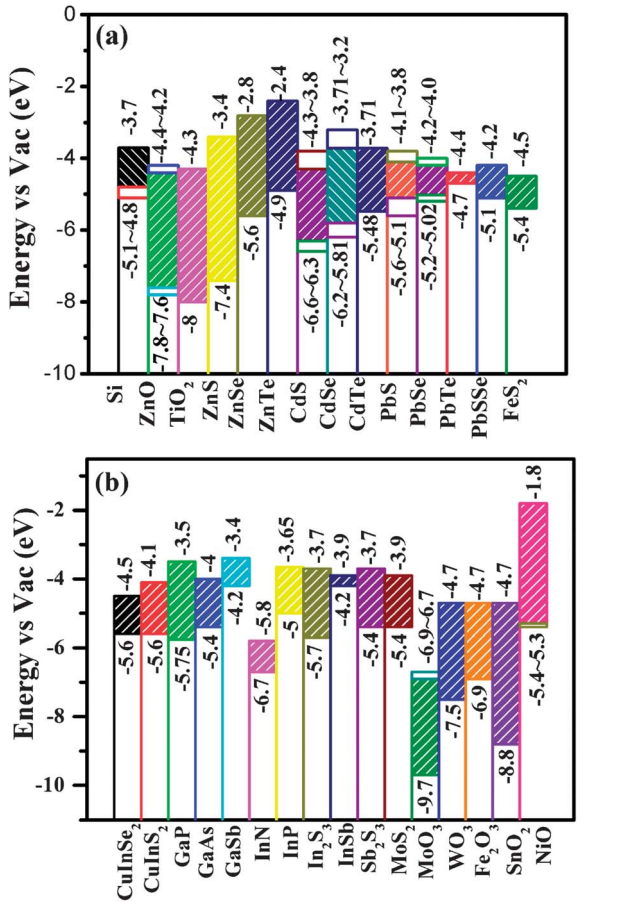

Fig. 4 Schematic of the energy bands of frequently used inorganics (a) and (b) in OIH solar cells.

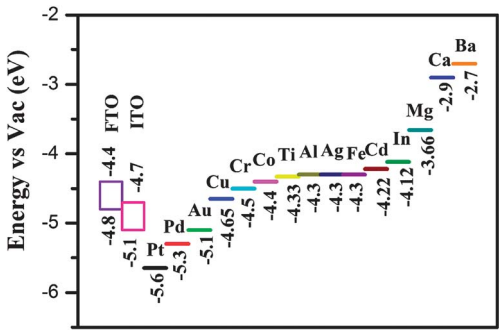

Fig. 5 Schematic of the energy band of the electrode materials used in OIH solar cells.

performance with a PCE of 6.56% because the negative shift of the P3HT Fermi level was favorable for building up a large internal electric field.[61] In contrast to the planar device with a PCE of 2.11%, OIH solar cells based on core–shell structures (Si nanopillar arrays/PbS quantum dots) have displayed a PCE of 6.53%.[62]

3 ZnO-based OIH solar cells

Due to its stability in air, facile synthesis and good light transmittance, ZnO has attracted extensive interest for use in OIH solar cells. OIH solar cells based on ZnO films, NCs and NRs/NWs have been summarized in detail.[63,64] Damage-free ZnO thin films on graphene/plastic substrates grown at a low

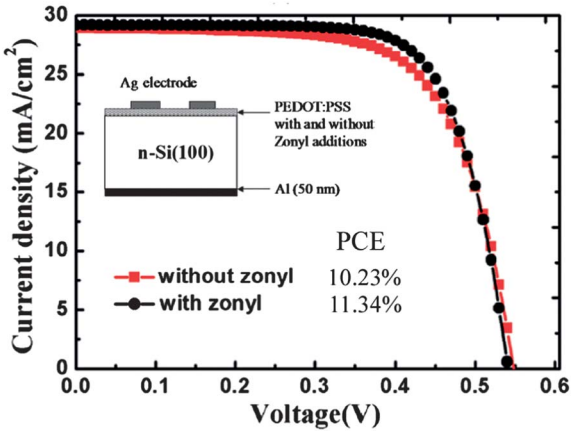

Fig. 6 Schematic structure and performance of a Si–PEDOT:PSS solar cell. Reproduced from ref. 30, AIP.

Table 2 The performances of Si and PEDOT:PSS solar cells with different interfaces and orientations. Reproduced from ref. 31, AIP

Sample	J_{sc} (mA cm^{-2})	V_{oc} (V)	FF (%)	PCE (%)
H–Si(111)	0.28	0.27	19.3	0.02
1.5 nm SiO_x–Si(111)	26.4	0.61	65.9	10.6
2.1 nm SiO_x–Si(111)	26.3	0.57	34.6	5.2
H–Si(100)	0.46	0.29	16.9	0.02
1.8 nm SiO_x–Si(100)	25.8	0.58	62.4	9.4
2.3 nm SiO_x–Si(100)	24.7	0.53	25.5	3.4

temperature of 160 °C have been used in a ZnO–PCBM–P3HT–MoO_3 solar cell and the PCE reached 1.55%.[65] In another work, a ZnO thin film was directly grown on a plastic substrates at 180 °C and the PCE reached 3.11%.[66] The PCE of a FTO–ZnO (60 nm NCs film)–Sb_2S_3 (100 nm)–P3HT (40 nm)–Ag OIH solar cell has approached 2.4%.[67] When ZnO NWs were included in the cell, the PCE increased to 2.9%.[68] The increased heterojunction area increased the exciton dissociation and resulted in an improved PCE. Octadecanethiol (ODT) and octadecyltriethoxysilane (OTES) are terminated with the same alkyl chain but different attachment groups. Surface treatment of polycrystalline ZnO films with ODT or OTES could enhance the P3HT polymer ordering. However, the PCE of a solar cell treated with ODT was improved from 0.076% for the untreated device to 0.139%, while the PCE decreased to 0.047% in the device treated with OTES. The surface dipoles associated with the two types of alkyl molecules resulted in this difference.[69] The dense ZnO film with a thickness of 173 nm was electrochemically deposited on ITO glass and the obtained PCE of the ITO–ZnO–PCBM–P3HT–WO_x cell was 4.91%.[70] OIH solar cells based on thin film ZnO and P3HT with/without modification exhibited PCEs in the range 0.03% to 0.35%.[71–75]

The PCE of a ZnO NCs–P3HT OIH solar cell reported by Janssen's group possessed the highest PCE of 2%.[76] Several approaches, such as surface modification, self-assembly with help of liquid crystal molecules or block copolymers, mixing with CdSe NCs, have been explored to improve the performance of solar cells. Their PCEs varied from 0.19% to 0.88%.[77–83] The Li-doped ZnO NCs could effectively enhance charge transfer at the interface of ZnO and P3HT because of the oxygen-enriched surface and suppression of charge injection from the electrode. The maximum PCE of 0.37% was obtained at a Li-doping concentration of 5 atom% .[84]

ZnO NW surfaces were modified with P3HT–didodecylquaterthiophene (P3HT/QT) to form core–shell junctions. The PCE of a single ZnO–P3HT nanowire was 0.036%, and a PCE of 0.033% was obtained from a single ZnO/QT nanowire device.[85] An OIH solar cell based on CuPC and fullerene combined with ZnO NWs had a PCE of 0.53%, which had a more than fourfold increase in performance than the device without ZnO NWs.[86] A PCE of 0.42% was achieved for an OIH solar cell composed of PbS QD coated ZnO NWs and MEH-PPV, which was increased almost 5 times compared with the solar cell without PbS QDs.[87] When CdS QDs were coated on the ZnO NRs in a ZnO–MEH-PPV cell, a maximum PCE of 0.65% was obtained.[88] An OIH solar cell consisting of CuPC and Al_2O_3 NPs-coated ZnO NRs possessed a PCE of 1.32%.[89] In a ZnO NW–P3HT OIH solar cell, TiO_2 NRs of diameter ~5 nm and length 20–30 nm were incorporated into polymers to facilitate charge separation and transport by providing an increased interfacial area and a more effective transport pathway, and a PCE of 0.59% has been achieved.[90] In a similar ZnO NW–P3HT cell, the introduction of graphene into polymer increased the PCE from 0.09% to 0.4%.[91] When a reduced graphene oxide (rGO) film was used as a transparent conductive coating, the exciton dissociation and charge collection in the ZnO NRs–P3HT OIH solar cell was improved with a PCE of 0.46%.[92] Graphene nanoflakes could greatly enhance charge extraction and carrier mobility in an OIH solar cell composed of P3HT:PCBM–ZnO NRs and the PCE was enhanced from 1.26% to 2.33%.[93] ZnO NWs treated with ammonia resulted in both better polymer infiltration inside the nanostructure and efficient carrier separation. In an Al–PEDOT:PSS–MDMO-PPV–ZnO–ITO cell, the PCE was improved from 0.02% to 0.29%, by nearly 15 times.[94] ZnO NRs modified with indoline dye demonstrated enhanced light-harvesting and charge-collecting properties in a ZnO–P3HT cell. The dipole moments directing away from the ZnO surface could suppress the reverse saturation dark current and charge recombination and the PCE was improved from 0.22% to 0.71%. Derivative squaraine molecules lead to the highest PCE of 1.02%.[95] A PCBM interlayer was inserted into the interface between the ZnO NRs and PCBM:P3HT, which caused enhanced optical absorption and reduced internal series resistance. The PCE was improved from 2.35% to 3.2% because of the interface modification.[96] After N719 dye modification of ZnO NRs, the PCE of an OIH solar cell consisting of ZnO NRs–PCBM:P3HT was increased from 1.16% to 2%.[97] The PCE of a ZnO NRs–PCBM:P3HT cell was improved from 1.6% to 2.6% as the thickness of the photoactive layer was increased from 240 nm to 350 nm, by slowing the spin coating rate of the photoactive layer.[98]

4 TiO_2-based OIH solar cells

Due to its high chemical stability, low cost, non-toxicity, strong photocatalytic activity and high photoelectric conversion

efficiency, TiO_2 has been extensively used in photovoltaic research. Nanostructured TiO_2, such as nanoporous films, NCs, NRs, NWs and NTs, have been utilized in dye-sensitized solar cells, heterojunction solar cells, photocatalysis, and many other applications.[99] An OIH solar cell was fabricated with *in situ* electropolymerization of PEDOT into a nanoporous TiO_2 film and a PCE of 0.09% was obtained.[100] Improved infiltration of MEH-PPV inside a nanoporous TiO_2 layer was realized by *in situ* chemical polymerization. Compared with the polymer synthesized *ex situ*, the photo-induced charge separation yield was improved by *in situ* polymerization and the PCE was increased from 0.038% to 0.063%.[101] OIH solar cells composed of P3HT–mesoporous TiO_2 with brookite and anatase crystalline phases gave reproducible PCEs of 0.48% and 0.74%.[102] A Mn-doped TiO_2 thin film has been used in a TiO_2–PCBM:P3HT solar cell and the highest obtained PCE was 2.44%.[103] Nanoporous TiO_2 films were prepared on conductive FTO glass using a polystyrene block poly(ethylene oxide) copolymer as the template. After CdS and CdSe QD co-sensitizing, an OIH solar cell based on 1.6 μm thick TiO_2 films could reach a PCE of 0.358%.[104] In an OIH solar cell composed of TiO_2/P3HT:PCBM, self-assembled molecules used to modify the TiO_2 surface with self-assembled monolayers could improve the device PCE from 2.8% to 3.8%. The SAM could reduce the recombination of charges, passivate inorganic surface trap states, and improve the exciton dissociation efficiency at the interface, as well as acting as a template to affect the polymer phases, morphology and crystals.[105] F8T2 and SFT2 were used as polymers in TiO_2 NCs film OIH solar cells and PCEs of 0.05% and 0.01% were obtained, respectively.[106]

Structure-directing agents provided opportunities to control the physicochemical interactions at TiO_2–MEH-PPV interfaces. The OIH solar cells exhibited improved photovoltaic properties with the highest PCE of 0.2%.[107] Self-assembled networks based on TiO_2 NCs and block copolymer poly(ethylene oxide)-*b*-polytriphenylamine as a structure directing agent were obtained by a one-pot synthesis. The solar cell performance was determined by the morphologies of the percolating networks and the best PCE was 0.11%.[108] The performance of OIH solar cells based on blending P3HT and different dye-modified TiO_2 NRs have been studied. The branched TiO_2 NRs exhibited superior performance to the linear TiO_2 NRs and the biggest improvement of PCE was from 0.05% to 0.16%.[109] OIH solar cells based on a blend of P3HT and TiO_2 NPs/NTs modified N719 dye were fabricated and the PCE was increased from 0.041% to 0.06% for NPs and 0.081% for NTs.[110] When an adequate amount of TiO_2 NRs were added to P3HT/TiO_2 NRs cells, charge separation and transport efficiency could be improved and an optimized PCE of 1.14% was obtained.[111] OIH solar cells based on P3HT and MoS_2 modified TiO_2 NCs with ~15 μm thick active layers exhibited a PCE of 1.3%.[112] The performance of P3HT/TiO_2 NRs was dependent on the morphology of the blend layer that could be determined by the molecular weight of P3HT, the solvent type, hybrid components, surface modification of TiO_2 NRs, the active layer thickness, the process conditions, and so on. A PCE of 0.83% was obtained with high molecular weight (65 kD) P3HT, the high boiling point solvent trichlorobenzene, and pyridine-modified TiO_2 NRs with an active layer thickness of ~100 nm.[113] The molecular weight of P3HT affected the interfacial morphology of the P3HT/TiO_2 NRs devices. The large domain structure from a polymer with a high molecular weight of 66 kD exhibited continuous absorption, as a result of enhanced polymer stacking and electronic delocalization. The PCE also reached 0.98%.[114] All solid-state OIH solar cells were fabricated by depositing Sb_2S_3 and P3HT on the surface of a mesoporous TiO_2 layer, where Sb_2S_3 acts as an absorbing semiconductor and P3HT acts as both the hole conductor and light absorber. A maximum PCE of 5.13% was obtained.[115] The Sb_2S_3 layer made the energy bands of the system match well over a wide absorption range, which produced a TiO_2 OIH solar cell with the highest PCE. In order to avoid organic solvents, all-water-solution-based PTEBS–TiO_2 solar cells have been demonstrated and the PCE could reach 0.17%.[116]

Highly ordered and vertically oriented TiO_2 NT arrays with a length of 250 nm and a diameter of 70 nm were prepared by atomic layer deposition coupled with anodic aluminum oxide template, schematically shown in Fig. 7. An ordered OIH solar cell was fabricated by infiltration of P3HT into the TiO_2 NTs and a PCE of 0.5% was obtained.[117] CdSe QDs were introduced as an interlayer in the P3HT–TiO_2 NR solar cells. The presence of CdSe QDs was found to provide enhanced light absorption, assisting the charge separation at the P3HT–TiO_2 interface, and leading to a low recombination rate of the electrons due to the stepwise structure of the band edge in P3HT–CdSe–TiO_2, which accounts for the observed enhanced photocurrent and

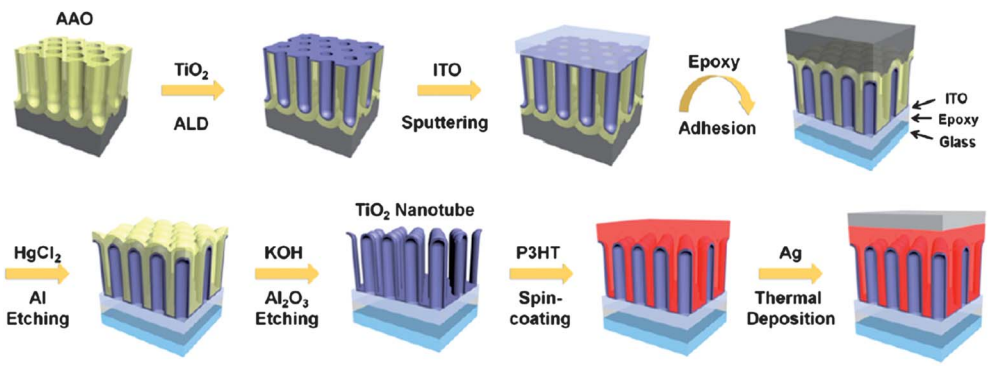

Fig. 7 Schematic of the fabrication process for OIH solar cells based on ordered TiO_2 NTs and P3HT. Reproduced from ref. 117, Elsevier.

photovoltage of the hybrid solar cells. As a result, the efficiency of the P3HT–CdSe QDs–TiO_2 NRs solar cell was greatly higher than that of the P3HT–TiO_2 NRs based cell.[118] The PCE of the OIH solar cell constructed from polymer coated TiO_2 NRs and P3HT reached 1.2% because of the enhanced electron mobility in the active layer interfaces. Moreover, the PCE decreased by less than 10% over 1000 h testing under ambient conditions without encapsulation.[119] An air-stable OIH solar cell comprised of Sb_2S_3 chemically deposited TiO_2 NWs to form coaxial Sb_2S_3–TiO_2 NWs and P3HT exhibited a maximum PCE of 4.65%.[120] The low cost surface modifiers could improve the polymer crystals, which could lead to efficient charge transport and reduced charge recombination. The PCE of an OIH solar cell consisting of surface-modified TiO_2 NRs and P3HT achieved 1.19%.[121] The PCE of OIH solar cells based on P3HT and electrospinning TiO_2 nanofibers was 0.59%. The interface modification could induce ordered backbone packing of the P3HT layer, low density of the trap states on the surface of TiO_2 and long lifetime of the carriers in the active layer, and the PCE reached 1.2%.[122] Insertion of organic dyes not only enhanced the absorption of sunlight, but also improved the exciton dissociation and carrier transportation in the TiO_2 NT arrays–/P3HT solar cell. The best PCEs approached 3.2%.[123]

5 II–VI semiconductor-based OIH solar cells

Except ZnO, other frequently used II–VI inorganic semiconductors will be discussed here. The higher photocurrents which were observed for P3HT–CdSe compared to MEH-PPV–CdSe were due to the hole mobilities of P3HT and MEH-PPV were 10^{-3} and 10^{-6} $cm^2\ V^{-1}\ s^{-1}$, respectively.[124] The PCE of the interfacially modified N719 dye CdS nanoporous film and P3HT solar cell was increased to 1.31% from 0.06% because N719 dye modification formed a dipole layer at the interface that modulated the interface energy level, reduced the interfacial charge recombination, and promoted exciton dissociation.[125] A tandem OIH solar cell consisting of a PbSe NC film and P3HT–PCBM bulk heterojunction film was fabricated. The PbSe layer worked as a photocurrent generator as well as a UV protector for the underlying polymer cell. The total PCE reached 2.5% and UV durability was demonstrated.[126]

The morphology of the PCPDTBT:CdSe blend was affected by the depositing solvent and post annealing in OIH solar cells based on CdSe NPs and PCPDTBT. When a solution processed ZnO NPs layer was inserted between the active layer and the metal cathode, the PCE of the cell was improved to 3.7% because the ZnO NP layer could block hole transporting to the cathode, extract electrons from the active layer, and shift the optical field distribution within the active layer for optimal absorption. Furthermore, the ZnO NP layer also results in a drastic improvement in the air stability of the hybrid solar cells with 70% of the original PCE retained after storage under ambient laboratory conditions for more than two months, compared to over 90% loss of PCE within several hours' exposure for similar devices without a ZnO NP layer.[127,128] Based on a CdSe QDs and PCPDTBT OIH solar cell, a maximum PCE of 2.8% was obtained by an annealing under 210 °C. When the elongated CdSe NRs were included, a maximum PCE of 3.6% was obtained because of the formation of a well-interconnected pathway for electrons within the p-type polymer matrix.[129] When the electro-attractive conjugated molecule F4TCNQ was used in the active layer of P3HT–CdSe QDs solar cells with a F4TCNQ:QDs weight ratio of 0.5%, the PCE could be improved by 2.3 times.[130] An OIH solar cell consisting of non-ligand-exchanged CdSe QDs and P3HT had an enhanced PCE of ~2%. After synthesis, the CdSe QDs are treated by a simple and fast acid-assisted washing procedure, which is a crucial factor in enhancing the device performance.[131] The incorporation of CdSe NPs in the PFT–PCBM mixture changed the film morphology and partially resulted in a performance improvement with a PCE of 1.3%.[132] The PCE of 3.2% was achieved in a conjugated polymer PCPDTBT and CdSe NPs OIH solar cell. The overall PCE increased with increasing incident light intensity and reached a maximum of 3.56%.[133] The CdSe : P3HT ratios of 8 : 1 to 10 : 1 were found to give the best results concerning the overall device performance.[134] A single axial heterojunction NW composed of CdS and PPY was successfully fabricated and exhibited a PCE of 0.018%.[135]

An *in situ* synthesis route for the fabrication of OIH solar cells involved mixing metal salts and thiourea, then thermally annealing to directly form metal sulfides in the polymer matrix. CdS–, PbS–, and ZnS–P3EBT composites with nanoscale phase separation have been demonstrated. A solar cell containing a CdS–P3EBT active layer exhibited a PCE of 0.06%.[136] CdS QDs were bound onto P3HT NWs through solvent-assisted grafting and ligand exchange, leading to controlled organic–inorganic phase separation and an improved PCE of 4.1%.[137] The *in situ* fabrication could form a good heterojunction interface and improve the crystallinity of the organic and inorganic components, which could enhance the exciton dissociation and carrier transportation and lead to an improved PCE. A P3HT–CdS NCs OIH solar cell was fabricated with a FTO-coated ZnO NR array as an electrode. The PCE of the cell was improved to 2.6% with 320 nm ZnO NRs on a 25 nm FTO layer and elongated CdS NCs with an aspect ratio of 4.[138] A general method has been developed to synthesize metal sulfide NP–polymer films at a low cost and low temperature which is compatible with large-scale device manufacturing. An OIH solar cell based on CdS–P3HT was demonstrated with *in situ* thermal decomposition of a solution processable precursor complex in a polymer film and a PCE of 0.7% was obtained.[139] In a CdS NP–P3HT hybrid cell, the PCE was improved from 0.06% to 0.3% when surface modified CdS NPs were incorporated.[140] It was found that the performance of the OIH solar cell was associated with the crystal facet of the inorganic component. In CdS/PEDOT:PSS, CdS/ZnPC and CdS/PANI:PSS cells, the PCE of the Cd-terminated surface was about double of that of S-terminated surface. The partial contribution was related to the specific interaction of the organic material with the surface atoms of the inorganic part.[141] Blending films containing P3HT and *in situ* grown CdS display a greater yield of photogenerated charges than a blend containing an equivalent amount of pre-synthesized CdS QDs.[142] Metal sulfide NP–polymer films were fabricated based on the controlled *in situ* thermal decomposition of a metal xanthate precursor complex in a solid-state polymer film. The demonstrated CdS–P3HT film exhibited

a PCE in excess of 2%.[143] An OIH solar cell based on the *in situ* growth of CdTe NCs in a P3HT matrix had a PCE of 0.79%.[144] *In situ* synthesized CdTe NPs could be easily dispersed in a MEH-PPV matrix. The OIH solar cell fabricated with 40 : 3 weight ratio of CdTe : MEH-PPV yielded a power conversion efficiency of 0.06%.[145] The P3HT–ZnS NP OIH solar cell has been demonstrated to be a portable device with low power consumption, which provided 1.20 V output voltage with a power density of 0.0024 mW cm^{-2}.[146]

An OIH solar cell composed of CdSe NR arrays vertically oriented to an ITO substrate and P3HT had an increased interface as well as facilitating charge transport. The PCE of the cell with a 3D interface was twice as large as that of another solar cell based on a bilayer thin film from 0.13% to 0.28%.[147] The vertically aligned CdS NRs provide the minimal electron transport path to reduce the charge carrier recombination at the heterojunction interface. The photoactive MEH-PPV layer was prepared by dip-/spin-coating and an optimal PCE of 0.035% was obtained.[148] OIH solar cells based on CdSe NR arrays and P3HT have been fabricated and the maximum PCE reached 1.38%.[149]

6 III–V semiconductor-based OIH solar cells

III–V inorganic semiconductors possess several unique properties and have been utilized to construct high efficiency third generation solar cells. Due to their relatively high cost, III–V semiconductors are frequently used in special fields or for a particular requirement. A few OIH solar cells based on III–V semiconductors have been summarized.[150] Solar cells based on PEDOT:PSS–n-GaN–sapphire (0001) and PANI–n-GaN–sapphire (0001) exhibited open-circuit voltages reaching 0.8 V and 0.73 V, respectively.[151] An OIH solar cell based on quercetin–p-InP has been fabricated *via* a solution-processing method at room temperature. The device exhibits strong photovoltaic behavior with a maximum open circuit voltage of 0.36 V.[152] In an OIH solar cell based on P3HT and GaAs NWs, coating the GaAs NWs with TiO_x shells could passivate the NW surface states and further improve the performance with an enhanced PCE of 2.36%.[153]

An air-stable PEDOT shell of controlled thickness was conformally grown on GaAs nanopillar arrays by electropolymerization. The properties of the organic layer could be readily tuned *in situ* and a PCE of 4.11% was achieved.[154] GaAs NW arrays were fabricated by dry etching with a monolayer of SiO_2 nanospheres as the etch mask. PEDOT:PSS conductive polymer was coated on the GaAs NW arrays to form an OIH solar cell. A maximum PCE of 5.8% was achieved, compared to only 0.3% PCE from the planar geometry solar cell, and this difference resulted from the large increase of heterojunction area.[155] OIH solar cells based on P3HT-coated GaAs nanopillars were grown on a patterned GaAs substrate using selective-area MOCVD. The hybrid solar cells had extremely low leakage currents and gave a PCE of 0.6%. Surface passivation of GaAs with ammonium sulfide resulted in a further improvement of the PCE to 1.44%.[156] The suppression of reflectance and the interpenetrating heterojunction interface of GaAs NW arrays offer an improvement in efficiency. Compared to the planar GaAs–PEDOT:PSS cells, the PCE was improved from 0.29% to 5.8%.[157]

7 Other inorganic-based OIH solar cells

Theoretical calculations revealed that InSb QDs or quantum wells should be optimal inorganics materials for use in OIH solar cells based on P3HT, which have a band gap of about 1.5 eV and HOMO level about 0.4 eV lower than P3HT. Moreover, chalcopyrite $MgSnSb_2$ quantum wells were predicted to be a cost-effective material for realizing high efficiency OIH solar cells.[158] An OIH solar cell consisting of cross-linked PbS NCs and a C_{60} layer improved the PCE to 2.2% because the C_{60} layer effectively prevents exciton quenching.[159] Incorporation of oxidized camphoric MWCNTs in P3HT could enhance hole transport, easily split excitons and suppress carrier recombination and the PCE of the P3OT/n-Si OIH solar cell was improved to 0.175%.[160] The introduction of metal NPs into OIH solar cells was expected to improve the exciton dissociation due to the strong electrical field at the metal–organic interface. Adding MWCNTs decorated with 20 wt% Pt NPs in n-Si–P3OT solar cells improved the PCE from 0.145% to 0.78%.[161] OIH solar cells based on the layered double hydroxide $Co_5(OH)_8(NO_3)_2 \cdot 2H_2O$ and P3BT were fabricated with a series of low-cost, low-temperature steps that are potentially adaptable for roll-to-roll processing or contact printing. The PCE of 0.0032% is presently far too low to be of practical use.[162]

The performance of the P3HT–$CuInSe_2$ OIH solar cells was affected by the weight ratios of mixture and the annealing temperature. The optimal device had a PCE of 0.07%.[163] An OIH solar cell based on a blend of $CuInS_2$ and C_{60} exhibited a PCE of 0.0008%.[164] $CuInS_2$ QDs with sizes of 2–4 nm have been successfully synthesized by a facile solvothermal approach with 4-bromothiophenol as the reduction and capping agent. The OIH solar cells based on the MEH-PPV–$CuInS_2$ QDs blends with a wide spectral response extending from 300 to 900 nm had a PCE of 0.128% at 470 nm.[165] Monovalent halide anions were used to enhance electronic transport and passivate surface defects in the PbS QDs films. Solar cells fabricated following this strategy show up to 6% PCE.[166] Phase segregation and continuous vertical phases of the PbS NCs and PCBM are obtained by simply cross-linking the composite film at room temperature for a few minutes. The size of the segregated domains could be adjusted with different weight ratios of PbS NCs and PCBM. A solar cell PCE of 3.7% was achieved.[167] OIH solar cells incorporating narrow band gap PbSSe NCs in P3HT were developed for the extensive use of solar radiation up to the near infrared range. The developed cell exhibited a large light-harvesting efficiency over a broad range, in which the external quantum efficiency reached 0.3% at 1100 nm.[168] Incorporation of inorganic NPs into P3HT–PCBM bulk heterojunction could enhance the solar cell performance. Cu_2S and CdSe of 4–5 nm diameter were introduced to a P3HT–PCBM mixture and the PCE was improved from 1.1 to 1.7% and from 3.5 to 4.3% respectively because of interface modification and matching of the energy bands.[169] In a blend of MDMO-PPV–pyridine-SnS_2 with a weight ratio of 50%, oleylamine ligands were coated on SnS_2 NPs and the PCE of the OIH solar cell reached 0.263%.[170] OIH solar cells comprising MDMO-PPV and SnS_2 NCs were prepared and a PCE of 0.148% was obtained.[171] In_2S_3 nanoflake

array structures could be fabricated *in situ* on ITO glass substrates through a one-step solvothermal treatment of an indium layer and sulfur powder in the presence of absolute ethanol. A preliminary OIH solar cell ITO–PEDOT:PSS–In_2S_3:P3HT–Al showed a PCE of 0.04%.[172] The environmentally friendly and low-cost FeS_2 NCs could extend absorption in the red light region up to 900 nm. The FeS_2 NCs of 10 nm diameter were homogeneously blended with P3HT to form an OIH solar cell with a PCE of 0.16%.[173]

8 Conclusion and perspectives

Based on up-to-date papers associated with OIH solar cells, some key issues have been discussed herein, including the energy band alignment of organic and inorganic materials, interfacial modification and control, and employing different kinds of nanostructures. According to the inorganic semiconductors frequently used in hybrid solar cells, six groups of popular OIH solar cells were summarized, including Si, ZnO, TiO_2, II–VI semiconductors, III–V semiconductors and others. The corresponding organic semiconductors are listed in Table 1. Energy bands of many organic, inorganic and metal components are schematically plotted in Fig. 3–5. In every group, all OIH solar cells were discussed in order with different interface configurations: planar film, blending with an active layer and ordered nanostructures. All the data in this article should be useful and interesting for readers concerned with solar cells and related optoelectronics fields.

Presently, several OIH solar cells have been fabricated which possess PCEs greater than 11% under laboratory conditions, which is attractive for practical applications. However, some concerns about lifetime, cost and flexibility have decreased interest in these materials for practical applications. Attention may be focused on the study of flexible and compatible OIH solar cells with special requirements, such as low-cost, portable, folding, integrated with clothes, or curtains, or mobile devices, or furniture, and so on. The balance between performance in practical applications and cost may be one of the important considerations for developments in the near future. In basic research, the heterojunction interface should be emphasized, by methods such as controlling modification, phase separation, decreasing trap states and increasing exciton dissociation. It is possible to further improve the PCE of OIH solar cells by these approaches.

Acknowledgements

The authors greatly acknowledge the support from the National Basic Research Program of China (973 Program) under the grant numbers 2012CB932401, 2010CB934700, and 2012CB934204, and the National Natural Science Foundation of China under the grant numbers 21101009, 20971010, 61076077, and 61274066, and the Research Fund for the Doctoral Program of Higher Education of China (Grant no. 20101102120051) and the Fundamental Research Funds for the Central Universities (Grant no. YWF-11-03 and no. YWF-11-03-Q-088).

References

1 M. A. Green, K. Emery, D. L. King, S. Igari and W. Warta, *Progr. Photovolt.: Res. Appl.*, 2001, **9**, 287–293.
2 D. E. Markov, C. Tanase, P. W. M. Blom and J. Wildeman, *Phys. Rev. B: Condens. Matter Mater. Phys.*, 2005, **72**, 045217.
3 D. E. Markov, E. Amsterdam, P. W. M. Blom, A. B. Sieval and J. C. Hummelen, *J. Phys. Chem. A*, 2005, **109**, 5266–5274.
4 J. J. M. Halls, K. Pichler, R. H. Friend, S. C. Moratti and A. B. Holmes, *Appl. Phys. Lett.*, 1996, **68**, 3120–3122.
5 G. Yu, J. Gao, J. C. Hummelen, F. Wudl and A. J. Heeger, *Science*, 1995, **270**, 1789–1791.
6 J. J. M. Halls, C. A. Walsh, N. C. Greenham, E. A. Marseglia, R. H. Friend, S. C. Moratti and A. B. Holmes, *Nature*, 1995, **376**, 498–500.
7 R. N. Marks, J. J. M. Halls, D. D. C. Bradley, R. H. Friend and A. B. Holmes, *J. Phys.: Condens. Matter*, 1994, **6**, 1379–1394.
8 S. Barth and H. Bassler, *Phys. Rev. Lett.*, 1997, **79**, 4445–4448.
9 H. T. Grahn, *Introduction to Semiconductor Physics*, World Scientific Publishing Company, Singapore, 1999.
10 B. R. Saunders, *J. Colloid Interface Sci.*, 2012, **369**, 1–15.
11 J. Chandrasekaran, D. Nithyaprakash, K. B. Ajjan, S. Maruthamuthu, D. Manoharan and S. Kumar, *Renewable Sustainable Energy Rev.*, 2011, **15**, 1228–1238.
12 M. Skompska, *Synth. Met.*, 2010, **160**, 1–15.
13 B. R. Saunders and M. L. Turner, *Adv. Colloid Interface Sci.*, 2008, **138**, 1–23.
14 E. Holder, N. Tessler and A. L. Rogach, *J. Mater. Chem.*, 2008, **18**, 1064–1078.
15 P. Reiss, E. Couderc, J. De Girolamo and A. Pron, *Nanoscale*, 2011, **3**, 446–489.
16 A. A. Damitha, T. Adikaari, D. M. Nanditha, M. Dissanayake, S. Ravi and P. Silva, *IEEE J. Sel. Top. Quantum Electron.*, 2010, **16**, 1595–1606.
17 S. Kumar and G. D. Scholes, *Microchim. Acta*, 2007, **160**, 315–325.
18 J. Boucle, P. Ravirajan and J. Nelson, *J. Mater. Chem.*, 2007, **17**, 3141–3153.
19 S. Guenes and N. S. Sariciftci, *Inorg. Chim. Acta*, 2008, **361**, 581–588.
20 H. L. Yip and A. K. Y. Jen, *Energy Environ. Sci.*, 2012, **5**, 5994–6011.
21 A. J. Moule, L. Chang, C. Thambidurai, R. Vidu and P. Stroeve, *J. Mater. Chem.*, 2012, **22**, 2351–2368.
22 L. Li, T. Zhai, H. Zeng, X. Fang, Y. Bando and D. Golberg, *J. Mater. Chem.*, 2011, **21**, 40–56.
23 M. Yu, Y. Z. Long, B. Sun and Z. Fan, *Nanoscale*, 2012, **4**, 2783–2796.
24 M. D. McGehee, *MRS Bull.*, 2011, **34**, 95–100.
25 F. Zhang, B. Sun, T. Song, X. Zhu and S. T. Lee, *Chem. Mater.*, 2011, **23**, 2084–2090.
26 D. H. Lin, S. C. Shiu, J. S. Huang and C. F. Lin, *IEEE Photovoltaic Spec. Conf., 34th*, 2010, 949–950.
27 E. C. Garnett, C. Peters, M. Brongersma, C. Yi and M. McGehee, *IEEE Photovoltaic Spec. Conf., 34th*, 2010, 934–938.

28 G. Kalita, S. Adhikari, H. R. Aryal, R. Afre, T. Soga, M. Sharon, W. Koichi and M. Umeno, *J. Phys. D: Appl. Phys.*, 2009, **42**, 115104.
29 T. Song, S. T. Lee and B. Q. Sun, *J. Mater. Chem.*, 2012, **22**, 4216–4232.
30 Q. Liu, M. Ono, Z. Tang, R. Ishikawa, K. Ueno and H. Shirai, *Appl. Phys. Lett.*, 2012, **100**, 183901.
31 L. He, C. Jiang, H. Wang, D. Lai and Rusli, *Appl. Phys. Lett.*, 2012, **100**, 073503.
32 C. H. Lin, S. Chattopadhyay, C. W. Hsu, M. H. Wu, W. C. Chen, C. T. Wu, S. C. Tseng, J. S. Hwang, J. H. Lee, C. W. Chen, C. H. Chen, L. C. Chen and K. H. Chen, *Adv. Mater.*, 2009, **21**, 759–763.
33 S. Avasthi, S. T. Lee, Y. L. Loo and J. C. Sturm, *Adv. Mater.*, 2011, **23**, 5762–5766.
34 S. E. Bourdo, V. Saini, J. Piron, I. Al-Brahim, C. Boyer, J. Rioux, V. Bairi, A. S. Biris and T. Viswanathan, *ACS Appl. Mater. Interfaces*, 2012, **4**, 363–368.
35 L. L. Vovchenko, L. Y. Matzui, V. V. Oliynyk and V. L. Launetz, *Mol. Cryst. Liq. Cryst.*, 2011, **535**, 179–188.
36 M. M. El-Nahass, H. S. Metwally, H. E. A. El-Sayed and A. M. Hassanien, *Synth. Met.*, 2011, **161**, 2253–2258.
37 T. Kim, J. H. Jeon, S. Han, D. K. Lee, H. Kim, W. Lee and K. Kim, *Appl. Phys. Lett.*, 2011, **98**, 183503.
38 C. Y. Liu and U. R. Kortshagen, *Nanoscale*, 2012, **4**, 3963–3968.
39 S. Ben Dkhil, R. Bourguiga, J. Davenas and D. Cornu, *Mater. Sci. Eng., B*, 2012, **177**, 173–179.
40 L. He, D. Lai, H. Wang, C. Jiang and Rusli, *Small*, 2012, **8**, 1664–1668.
41 M. L. Zhang, I. Mahmood, X. Fan, G. Xu and N. B. Wong, *J. Nanosci. Nanotechnol.*, 2010, **10**, 8271–8277.
42 Y. Ma, F. Liu, M. Zhu and Z. Zhang, *Phys. Status Solidi C*, 2010, **7**, 537–540.
43 Y. Ma, F. Liu, M. zhu, J. Liu, Y. Yang, Y. Li and Z. Zhang, *EEE Photovoltaic Spec. Conf., 34th*, 2009, 000626–000628.
44 C. Y. Kuo and C. Gau, *Appl. Phys. Lett.*, 2009, **95**, 053302.
45 J. S. Huang, C. Y. Hsiao, S. J. Syu, J. J. Chao and C. F. Lin, *Sol. Energy Mater. Sol. Cells*, 2009, **93**, 621–624.
46 A. Nahor, O. Berger, Y. Bardavid, G. Toker, Y. Tamar, L. Reiss, M. Asscher, S. Yitzchaik and A. Sa'ar, *Phys. Status Solidi C*, 2011, **8**, 1908–1912.
47 S. C. Shiu, J. J. Chao, S. C. Hung, C. L. Yeh and C. F. Lin, *Chem. Mater.*, 2010, **22**, 3108–3113.
48 F. Zhang, T. Song and B. Sun, *Nanotechnology*, 2012, **23**, 194006.
49 H. J. Syu, S. C. Shiu and C. F. Lin, *Sol. Energy Mater. Sol. Cells*, 2012, **98**, 267–272.
50 L. He, C. Jiang, H. Wang, D. Lai, Y. H. Tan, C. S. Tan and Rusli, *Appl. Phys. Lett.*, 2012, **100**, 103104.
51 B. Ozdemir, M. Kulakci, R. Turan and H. E. Unalan, *Appl. Phys. Lett.*, 2011, **99**, 113510.
52 L. He, C. Jiang, H. Wang, D. Lai and Rusli, *ACS Appl. Mater. Interfaces*, 2012, **4**, 1704–1708.
53 L. He, C. Jiang, Rusli, D. Lai and H. Wang, *Appl. Phys. Lett.*, 2011, **99**, 021104.
54 X. Shen, B. Sun, D. Liu and S. T. Lee, *J. Am. Chem. Soc.*, 2011, **133**, 19408–19415.
55 S. A. Moiz, A. M. Nahhas, H. D. Um, S. W. Jee, H. K. Cho, S. W. Kim and J. H. Lee, *Nanotechnology*, 2012, **23**, 145401.
56 W. Lu, Q. Chen, B. Wang and L. Chen, *Appl. Phys. Lett.*, 2012, **100**, 023112.
57 S. Jeong, E. C. Garnett, S. Wang, Z. Yu, S. Fan, M. L. Brongersma, M. D. McGehee and Y. Cui, *Nano Lett.*, 2012, **12**, 2971–2976.
58 F. Zhang, X. Han, S. T. Lee and B. Sun, *J. Mater. Chem.*, 2012, **22**, 5362–5368.
59 Z. Pei, S. Thiyagu, M. S. Jhong, W. S. Hsieh, S. J. Cheng, M. W. Ho, Y. H. Chen, J. C. Liu and C. M. Yeh, *Sol. Energy Mater. Sol. Cells*, 2011, **95**, 2431–2436.
60 L. He, Rusli, C. Jiang, H. Wang and D. Lai, *IEEE Electron Device Lett.*, 2011, **32**, 1406–1408.
61 X. F. Lei, F. Zhang, T. Song and B. Q. Sun, *Appl. Phys. Lett.*, 2011, **99**, 233305.
62 T. Song, F. Zhang, X. F. Lei, Y. L. Xu, S. T. Lee and B. Q. Sun, *Nano Energy*, 2012, **4**, 1336–1343.
63 J. W. P. Hsu and M. T. Lloyd, *MRS Bull.*, 2011, **35**, 422–428.
64 J. Huang, Z. Yin and Q. Zheng, *Energy Environ. Sci.*, 2011, **4**, 3861–3877.
65 K. S. Shin, H. Jo, H. J. Shin, W. M. Choi, J. Y. Choi and S. W. Kim, *J. Mater. Chem.*, 2012, **22**, 13032–13038.
66 K. S. Shin, H. J. Park, B. Kumar, K. K. Kim, S. G. Ihn and S. W. Kim, *J. Mater. Chem.*, 2011, **21**, 12274–12279.
67 C. P. Liu, H. E. Wang, T. W. Ng, Z. H. Chen, W. F. Zhang, C. Yan, Y. B. Tang, I. Bello, L. Martinu, W. J. Zhang and S. K. Jha, *Phys. Status Solidi B*, 2012, **249**, 627–633.
68 C. P. Liu, Z. H. Chen, H. E. Wang, S. K. Jha, W. J. Zhang, I. Bello and J. A. Zapien, *Appl. Phys. Lett.*, 2012, **100**, 243102.
69 C. G. Allen, D. J. Baker, T. M. Brenner, C. C. Weigand, J. M. Albin, K. X. Steirer, D. C. Olson, C. Ladam, D. S. Ginley, R. T. Collins and T. E. Furtak, *J. Phys. Chem. C*, 2012, **116**, 8872–8880.
70 S. Schumann, R. Da Campo, B. Illy, A. C. Cruickshank, M. A. McLachlan, M. P. Ryan, D. J. Riley, D. W. McComb and T. S. Jones, *J. Mater. Chem.*, 2011, **21**, 2381–2386.
71 B. R. Lee, H. Choi, J. SunPark, H. J. Lee, S. O. Kim, J. Y. Kim and M. H. Song, *J. Mater. Chem.*, 2011, **21**, 2051–2053.
72 R. J. Davis, M. T. Lloyd, S. R. Ferreira, M. J. Bruzek, S. E. Watkins, L. Lindell, P. Sehati, M. Fahlman, J. E. Anthony and J. W. P. Hsu, *J. Mater. Chem.*, 2011, **21**, 1721–1729.
73 Y. Vaynzof, D. Kabra, L. Zhao, P. K. H. Ho, A. T. S. Wee and R. H. Friend, *Appl. Phys. Lett.*, 2010, **97**, 033309.
74 J. Boucle, H. J. Snaith and N. C. Greenham, *J. Phys. Chem. C*, 2010, **114**, 3664–3674.
75 M. T. Lloyd, R. P. Prasankumar, M. B. Sinclair, A. C. Mayer, D. C. Olson and J. W. P. Hsu, *J. Mater. Chem.*, 2009, **19**, 4609–4614.
76 S. D. Oosterhout, M. M. Wienk, S. S. van Bavel, R. Thiedmann, L. J. A. Koster, J. Gilot, J. Loos, V. Schmidt and R. A. J. Janssen, *Nat. Mater.*, 2009, **8**, 818–824.
77 K. Yuan, F. Li, L. Chen, Y. Li and Y. Chen, *J. Phys. Chem. C*, 2012, **116**, 6332–6339.
78 K. Yao, L. Chen, Y. Chen, F. Li and P. Wang, *J. Phys. Chem. C*, 2012, **116**, 3486–3491.

79 J. Yang, L. Qian, R. Zhou, Y. Zheng, A. Tang, P. H. Holloway and J. Xue, *J. Appl. Phys.*, 2012, **111**, 044323.
80 W. Chen, Y. Chen, F. Li, L. Chen, K. Yuan, K. Yao and P. Wang, *Sol. Energy Mater. Sol. Cells*, 2012, **96**, 266–275.
81 K. Yuan, F. Li, Y. Chen, X. Wang and L. Chen, *J. Mater. Chem.*, 2011, **21**, 11886–11894.
82 H. R. Tan, X. W. Zhang, F. R. Tan, H. L. Gao, Z. G. Yin, Y. M. Bai, X. L. Zhang and S. C. Qu, *Phys. Status Solidi A*, 2011, **208**, 2865–2870.
83 S. Zhang, C. I. Pelligra, G. Keskar, J. Jiang, P. W. Majewski, A. D. Taylor, S. Ismail-Beigi, L. D. Pfefferle and C. O. Osuji, *Adv. Mater.*, 2012, **24**, 82–87.
84 P. Ruankham, T. Sagawa, H. Sakaguchi and S. Yoshikawa, *J. Mater. Chem.*, 2011, **21**, 9710–9715.
85 A. L. Briseno, T. W. Holcombe, A. I. Boukai, E. C. Garnett, S. W. Shelton, J. J. M. Freacutechet and P. Yang, *Nano Lett.*, 2010, **10**, 334–340.
86 J. Liu, S. Wang, Z. Bian, M. Shan and C. Huang, *Appl. Phys. Lett.*, 2009, **94**, 173107.
87 L. Wang, D. Zhao, Z. Su and D. Shen, *Nanoscale Res. Lett.*, 2012, **7**, 1–6.
88 L. Wang, D. Zhao, Z. Su, B. Li, Z. Zhang and D. Shen, *J. Electrochem. Soc.*, 2011, **158**, H804–H807.
89 S. C. Lin, S. Y. Chen and C. H. Peng, *J. Nanosci. Nanotechnol.*, 2010, **10**, 4602–4606.
90 Y. Y. Lin, C. W. Chen, T. H. Chu, W. F. Su, C. C. Lin, C. H. Ku, J. J. Wu and C. H. Chen, *J. Mater. Chem.*, 2007, **17**, 4571–4576.
91 S. AbdulAlmohsin and J. B. Cui, *J. Phys. Chem. C*, 2012, **116**, 9433–9438.
92 K. Yang, C. Xu, L. Huang, L. Zou and H. Wang, *Nanotechnology*, 2011, **22**, 405401.
93 Y. M. Sung, F. C. Hsu, D. Y. Wang, I. S. Wang, C. C. Chen, H. C. Liao, W. F. Su and Y. F. Chen, *J. Mater. Chem.*, 2011, **21**, 17462–17467.
94 S. Pradhan, S. Karak and A. Dhar, *J. Phys. D: Appl. Phys.*, 2012, **45**, 235104.
95 P. Ruankham, L. Macaraig, T. Sagawa, H. Nakazumi and S. Yoshikawa, *J. Phys. Chem. C*, 2011, **115**, 23809–23816.
96 J. S. Huang, C. Y. Chou and C. F. Lin, *Sol. Energy Mater. Sol. Cells*, 2010, **94**, 182–186.
97 R. Thitima, C. Patcharee, S. Takashi and Y. Susumu, *Solid-State Electron.*, 2009, **53**, 176–180.
98 J. S. Huang, C. Y. Chou, M. Y. Liu, C. H. Wu, Y. H. Lin, W. H. Lin and C. F. Lin, *Proc. SPIE–Int. Soc. Opt. Eng.*, 2009, **7416**, 74161H1–9.
99 J. Yan and F. Zhou, *J. Mater. Chem.*, 2011, **21**, 9406–9418.
100 J. Dehaudt, L. Beouch, S. Peralta, C. Plesse, P. H. Aubert, C. Chevrot and F. Goubard, *Thin Solid Films*, 2011, **519**, 1876–1881.
101 P. Atienzar, T. Ishwara, M. Horie, J. R. Durrant and J. Nelson, *J. Mater. Chem.*, 2009, **19**, 5377–5380.
102 E. Lancelle-Beltran, P. Prene, C. Boscher, P. Belleville, P. Buvat, S. Lambert, F. Guillet, C. Marcel and C. Sanchez, *Eur. J. Inorg. Chem.*, 2008, 903–910.
103 Z. Alparslan, A. Kosemen, O. Ornek, Y. Yerli and S. E. San, *Int. J. Photoenergy*, 2011, **2011**, 734618.
104 Z. Liu, Y. Li, Z. Zhao, Y. Cui, K. Hara and M. Miyauchi, *J. Mater. Chem.*, 2010, **20**, 492–497.
105 S. K. Hau, H. L. Yip, O. Acton, N. S. Baek, H. Ma and A. K. Y. Jen, *J. Mater. Chem.*, 2008, **18**, 5113–5119.
106 J. Jo, D. Vak, Y. Y. Noh, S. S. Kim, B. Lim and D. Y. Kim, *J. Mater. Chem.*, 2008, **18**, 654–659.
107 S. Neyshtadt, J. P. Jahnke, R. J. Messinger, A. Rawal, T. S. Peretz, D. Huppert, B. F. Chmelka and G. L. Frey, *J. Am. Chem. Soc.*, 2011, **133**, 10119–10133.
108 M. C. Lechmann, S. A. L. Weber, J. Geserick, N. Husing, R. Berger and J. S. Gutmann, *J. Mater. Chem.*, 2011, **21**, 7765–7770.
109 J. Luo, C. Liu, S. Yang and Y. Cao, *Sol. Energy Mater. Sol. Cells*, 2010, **94**, 501–508.
110 Z. J. Wang, S. C. Qu, X. B. Zeng, J. P. Liu, C. S. Zhang, F. R. Tan, L. Jin and Z. G. Wang, *Appl. Surf. Sci.*, 2008, **255**, 1916–1920.
111 C. H. Chang, T. K. Huang, Y. T. Lin, Y. Y. Lin, C. W. Chen, T. H. Chu and W. F. Su, *J. Mater. Chem.*, 2008, **18**, 2201–2207.
112 M. Shanmugam, T. Bansal, C. A. Durcan and B. Yu, *Appl. Phys. Lett.*, 2012, **100**, 153901.
113 T. W. Zeng, H. H. Lo, C. H. Chang, Y. Y. Lin, C. W. Chen and W. F. Su, *Sol. Energy Mater. Sol. Cells*, 2009, **93**, 952–957.
114 M. C. Wu, C. H. Chang, H. H. Lo, Y. S. Lin, Y. Y. Lin, W. C. Yen, W. F. Su, Y. F. Chen and C. W. Chen, *J. Mater. Chem.*, 2008, **18**, 4097–4102.
115 J. A. Chang, J. H. Rhee, S. H. Im, Y. H. Lee, H. J. Kim, S. I. Seok, M. K. Nazeeruddin and M. Gratzel, *Nano Lett.*, 2010, **10**, 2609–2612.
116 Q. Qiao, Y. Xie and J. T. McLeskey, *J. Phys. Chem. C*, 2008, **112**, 9912–9916.
117 J. Lee and J. Y. Jho, *Sol. Energy Mater. Sol. Cells*, 2011, **95**, 3152–3156.
118 J. Wang, T. Zhang, D. Wang, R. Pan, Q. Wang and H. Xia, *Chem. Phys. Lett.*, 2012, **541**, 105–109.
119 H. C. Liao, C. H. Lee, Y. C. Ho, M. H. Jao, C. M. Tsai, C. M. Chuang, J. J. Shyue, Y. F. Chen and W. F. Su, *J. Mater.Chem.*, 2012, **22**, 10589–10596.
120 J. C. Cardoso, C. A. Grimes, X. Feng, X. L. Zhang, S. Komarneni, M. V. B. Zanoni and N. Bao, *Chem. Commun.*, 2012, **48**, 2818–2820.
121 Y. C. Huang, J. H. Hsu, Y. C. Liao, W. C. Yen, S. S. Li, S. T. Lin, C. W. Chen and W. F. Su, *J. Mater. Chem.*, 2011, **21**, 4450–4456.
122 Q. Tai, X. Zhao and F. Yan, *J. Mater. Chem.*, 2010, **20**, 7366–7371.
123 S. Kim, G. K. Mor, M. Paulose, O. K. Varghese, K. Shankar and C. A. Grimes, *IEEE J. Sel. Top. Quantum Electron.*, 2010, **16**, 1573–1580.
124 S. Biswas, Y. Li, M. A. Stroscio and M. Dutta, *J. Appl. Phys.*, 2012, **111**, 044313.
125 M. Zhong, D. Yang, J. Zhang, J. Shi, X. Wang and C. Li, *Sol. Energy Mater. Sol. Cells*, 2012, **96**, 160–165.
126 S. J. Kim, W. J. Kim, A. N. Cartwright and P. N. Prasad, *Sol. Energy Mater. Sol. Cells*, 2009, **93**, 657–661.
127 R. Zhou, Y. Zheng, L. Qian, Y. Yang, P. H. Holloway and J. Xue, *Nanoscale*, 2012, **4**, 3507–3514.

128 L. Qian, J. Yang, R. Zhou, A. Tang, Y. Zheng, T. K. Tseng, D. Bera, J. Xue and P. H. Holloway, *J. Mater. Chem.*, 2011, **21**, 3814–3817.
129 K. F. Jeltsch, M. Schaedel, J. B. Bonekamp, P. Niyamakom, F. Rauscher, H. W. A. Lademann, I. Dumsch, S. Allard, U. Scherf and K. Meerholz, *Adv. Funct. Mater.*, 2012, **22**, 397–404.
130 M. Boivin, S. Lamarre, J. Tessier, M. Lecavalier, A. Najari, S. Dufour-Beausejour, E. B. Dussault, P. Collin and C. N. Allen, *Appl. Phys. Lett.*, 2012, **100**, 033302.
131 Y. Zhou, F. S. Riehle, Y. Yuan, H. F. Schleiermacher, M. Niggemann, G. A. Urban and M. Krueger, *Appl. Phys. Lett.*, 2010, **96**, 013304.
132 J. N. de Freitas, I. R. Grova, L. C. Akcelrud, E. Arici, N. S. Sariciftci and A. F. Nogueira, *J. Mater. Chem.*, 2010, **20**, 4845–4853.
133 S. Dayal, N. Kopidakis, D. C. Olson, D. S. Ginley and G. Rumbles, *Nano Lett.*, 2010, **10**, 239–242.
134 F. Zutz, I. Lokteva, N. Radychev, J. Kolny-Olesiak, I. Riedel, H. Borchert and J. Parisi, *Phys. Status Solidi A*, 2009, **206**, 2700–2708.
135 Y. Guo, Y. Zhang, H. Liu, S. W. Lai, Y. Li, Y. Li, W. Hu, S. Wang, C. M. Che and D. Zhu, *J. Phys. Chem. Lett.*, 2010, **1**, 327–330.
136 E. Maier, A. Fischereder, W. Haas, G. Mauthner, J. Albering, T. Rath, F. Hofer, E. J. W. List and G. Trimmel, *Thin Solid Films*, 2011, **519**, 4201–4206.
137 S. Ren, L. Y. Chang, S. K. Lim, J. Zhao, M. Smith, N. Zhao, V. Bulovic, M. Bawendi and S. Gradecak, *Nano Lett.*, 2011, **11**, 3998–4002.
138 H. C. Liao, C. C. Lin, Y. W. Chen, T. C. Liu and S. Y. Chen, *J. Mater. Chem.*, 2010, **20**, 5429–5435.
139 H. C. Leventis, S. P. King, A. Sudlow, M. S. Hill, K. C. Molloy and S. A. Haque, *Nano Lett.*, 2010, **10**, 1253–1258.
140 A. Guchhait and A. J. Pal, *J. Phys. Chem. C*, 2010, **114**, 19294–19298.
141 O. P. Dimitriev, V. V. Kislyuk, A. F. Syngaevsky, P. S. Smertenko and A. A. Pud, *Phys. Status Solidi A*, 2009, **206**, 2645–2651.
142 L. X. Reynolds, T. Lutz, S. Dowland, A. MacLachlan, S. King and S. A. Haque, *Nanoscale*, 2012, **4**, 1561–1564.
143 S. Dowland, T. Lutz, A. Ward, S. P. King, A. Sudlow, M. S. Hill, K. C. Molloy and S. A. Haque, *Adv. Mater.*, 2011, **23**, 2739–2744.
144 M. T. Khan, A. Kaur, S. K. Dhawan and S. Chand, *J. Appl. Phys.*, 2011, **110**, 044509.
145 D. Verma, A. R. Rao and V. Dutta, *Sol. Energy Mater. Sol. Cells*, 2009, **93**, 1482–1487.
146 M. Bredol, K. Matras, A. Szatkowski, J. Sanetra and A. Prodi-Schwab, *Sol. Energy Mater. Sol. Cells*, 2009, **93**, 662–666.
147 S. Kwon, M. Shim, J. I. Lee, T. W. Lee, K. Cho and J. K. Kim, *J. Mater. Chem.*, 2011, **21**, 12449–12453.
148 X. Jiang, F. Chen, H. Xu, L. Yang, W. Qiu, M. Shi, M. Wang and Z. Chen, *Sol. Energy Mater. Sol. Cells*, 2010, **94**, 338–344.
149 M. Schierhorn, S. W. Boettcher, J. H. Peet, E. Matioli, G. C. Bazan, G. D. Stucky and M. Moskovits, *ACS Nano*, 2010, **4**, 6132–6136.
150 P. L. Ong and I. A. Levitsky, *Energies*, 2010, **3**, 313–334.
151 N. Matsuki, Y. Irokawa, Y. Nakano and M. Sumiya, *Sol. Energy Mater. Sol. Cells*, 2011, **95**, 284–287.
152 O. Guellue and A. Tueruet, *Sol. Energy Mater. Sol. Cells*, 2008, **92**, 1205–1210.
153 S. Ren, N. Zhao, S. C. Crawford, M. Tambe, V. Bulovic and S. Gradecak, *Nano Lett.*, 2011, **11**, 408–413.
154 G. Mariani, Y. Wang, P. S. Wong, A. Lech, C. H. Hung, J. Shapiro, S. Prikhodko, M. El-Kady, R. B. Kaner and D. L. Huffaker, *Nano Lett.*, 2012, **12**, 3581–3586.
155 J. J. Chao, S. C. Shiu, S. C. Hung and C. F. Lin, *Proc. SPIE–Int.Soc. Opt. Eng.*, 2011, **8111**, 81110V1–6.
156 G. Mariani, R. B. Laghumavarapu, B. T. de Villers, J. Shapiro, P. Senanayake, A. Lin, B. J. Schwartz and D. L. Huffaker, *Appl. Phys. Lett.*, 2010, **97**, 013107.
157 J. J. Chao, S. C. Shiu, S. C. Hung and C. F. Lin, *Nanotechnology*, 2010, **21**, 285203.
158 H. Xiang, S. H. Wei and X. Gong, *J. Phys. Chem. C*, 2009, **113**, 18968–18972.
159 S. W. Tsang, H. Fu, R. Wang, J. Lu, K. Yu and Y. Tao, *Appl. Phys. Lett.*, 2009, **95**, 183505.
160 S. P. Somani, P. R. Somani and M. Umeno, *Diamond Relat. Mater.*, 2008, **17**, 585–588.
161 P. R. Somani, S. P. Somani and M. Umeno, *Appl. Phys. Lett.*, 2008, **93**, 033315.
162 B. Schwenzer, J. R. Neilson, K. Sivula, C. Woo, J. M. J. Frehet and D. E. Morse, *Thin Solid Films*, 2009, **517**, 5722–5727.
163 Y. Yang, H. Zhong, Z. Bai, B. Zou, Y. Li and G. D. Scholes, *J. Phys. Chem. C*, 2012, **116**, 7280–7286.
164 A. Tareda, T. Oku, A. Suzuki, K. Kikuchi and S. Kikuchi, *J. Ceram. Soc. Jpn.*, 2009, **117**, 967–969.
165 W. Yue, S. Han, R. Peng, W. Shen, H. Geng, F. Wu, S. Tao and M. Wang, *J. Mater. Chem.*, 2010, **20**, 7570–7578.
166 J. Tang, K. W. Kemp, S. Hoogland, K. S. Jeong, H. Liu, L. Levina, M. Furukawa, Wang, R. Debnath, D. Cha, K. W. Chou, A. Fischer, A. Amassian, J. B. Asbury and E. H. Sargent, *Nat. Mater.*, 2011, **10**, 765–771.
167 S. W. Tsang, H. Fu, J. Ouyang, Y. Zhang, K. Yu, J. Lu and Y. Tao, *Appl. Phys. Lett.*, 2010, **96**, 243104.
168 M. Nam, S. Kim, T. Kim, S. W. Kim and K. K. Lee, *Appl. Phys. Lett.*, 2011, **99**, 233115.
169 H. C. Liao, C. S. Tsao, T. H. Lin, M. H. Jao, C. M. Chuang, S. Y. Chang, Y. C. Huang, Y. T. Shao, C. Y. Chen, C. J. Su, U. S. Jeng, Y. F. Chen and W. F. Su, *ACS Nano*, 2012, **6**, 1657–1666.
170 F. R. Tan, S. C. Qu, J. Wu, K. Liu, S. Zhou and Z. G. Wang, *Nanoscale Res. Lett.*, 2011, **6**, 298–8.
171 F. R. Tan, S. Qu, X. B. Zeng, C. S. Zhang, M. Shi, Z. Wang, L. Jin, Y. Bi, J. Cao, Z. G. Wang, Y. Hou, F. Teng and Z. Feng, *Solid State Commun.*, 2010, **150**, 58–61.
172 H. Jia, W. He, X. Chen, Y. Lei and Z. Zheng, *J. Mater. Chem.*, 2011, **21**, 12824–12828.
173 Y. Y. Lin, D. Y. Wang, H. C. Yen, H. L. Chen, C. C. Chen, C. M. Chen, C. Y. Tang and C. W. Chen, *Nanotechnology*, 2009, **20**, 405207.